Phys Chem Minerals (1998) 25:112–121

ORIGINAL PAPER

Ph. Ildefonse · D. Cabaret · Ph. Sainctavit · G. Calas
A.-M. Flank · P. Lagarde

Aluminium X-ray absorption Near Edge Structure in model compounds and Earth's surface minerals

Received: 18 December 1996 / Revised, accepted: 2 June 1997

Abstract Aluminium K-edge X-ray absorption near edge spectra (XANES) of a suite of silicate and oxides minerals consist of electronic excitations occurring in the edge region, and multiple scattering resonances at higher energies. The main XANES feature for four-fold Al is at around 2 eV lower energy than the main XANES feature for six-fold Al. This provides a useful probe for coordination numbers in clay minerals, gels, glasses or material with unknown Al-coordination number. Six-fold aluminium yields a large variety of XANES features which can be correlated with octahedral point symmetry, number of aluminium sites and distribution of Al-O distances. These three parameters may act together, and the quantitative interpretation of XANES spectra is difficult. For a low point symmetry (1), variations are mainly related to the number of Al sites and distribution of Al-O distances: pyrophyllite, one Al site, is clearly distinguished from kaolinite and gibbsite presenting two Al sites. For a given number of Al-site (1), variations are controlled by changes in point symmetry, the number of XANES features being increased as point symmetry decreases. For a given point symmetry (1) and a given number of Al site (1), variations are related to second nearest neighbours (gibbsite versus kaolinite). The amplitude of the XANES feature at about 1566 eV is a useful probe for the assessment of Al^{IV}/Al^{total} ratios in 2/1 phyllosilicates. Al-K XANES has been performed on synthetic Al-bearing goethites which cannot be studied by ^{27}Al NMR. At low Al content, Al-K XANES is very different from that of α-AlOOH but at the highest level, XANES spectrum tends to that of diaspore. Al-K XAS is thus a promising tool for the structural study of poorly ordered materials such as clay minerals and natural alumino-silicate gels together with Al-subsituted Fe-oxyhydroxides.

Ph. Ildefonse (✉) · D. Cabaret · Ph. Sainctavit · G. Calas
Laboratoire de Minéralogie-Cristallographie, UA CNRS 09,
Universités Paris 6 et 7, and IPGP 4 place Jussieu,
75252 Paris cedex 05
Fax 33(0) 1 44 27 37 85; e-mail: ildefons@lmcp.jussieu.fr

Ph. Sainctavit · A.-M. Flank · P. Lagarde
LURE, CNRS/CEA/MEN, Bat. 209D, 91405 Orsay

Introduction

Aluminium is an abundant element at the Earth's surface and a major constituent in many low temperature alteration and weathering minerals. It also occurs as a minor element in iron oxyhydroxides. The Al coordination number (CN) is a major parameter governing the formation and stability of low-temperature weathering minerals, and inter-site distribution is often derived from calculations based on chemical analysis using structural models. In near-surface environments, aluminium is mainly six-fold coordinated to oxygen, and the local structure of this octahedral environment is difficult to assess by conventional X-ray diffraction methods, because most clay minerals are poorly crystallized or have significant stacking disorder, which gives them a two-dimensional character. In this situation, X-ray diffraction is not sensitive to short-range structure or to the local environment of a specific element. In addition, compounds that do not exhibit X-ray diffraction peaks are frequently encountered in near surface environments: iron and alumino-silicate gels in soils, lake sediments and stream deposits. Structural characterization of the cation sites in these amorphous materials is not possible using classical X-ray scattering methods (Ildefonse et al. 1994).

Spectroscopic methods are often highly sensitive to the local cation environment. Local Al environments have been extensively studied by ^{27}Al NMR spectroscopy (see Kirkpatrick 1988 for an overview). The use of ^{27}Al NMR is however limited, because the samples must have a low content of paramagnetic components. X-ray absorption spectroscopy (XAS) is element specific and yields information about the local environments of the probed atom (Brown and Parks 1989) and it is not dependent on the absence of paramagnetic impurities. XAS is commonly subdivided into two regions, Extended X-ray Absorption Fine Structure (EXAFS, see Galoisy et al. 1995, for short range influence) and X-ray Absorption Near-Edge Structure (XANES, see Cabaret et al. 1996, for medium range influence) spectroscopy. XANES spectroscopy can pro-

vide information about the oxidation state of an atom (Calas and Petiau 1983; Waychunas et al. 1983; Wong et al. 1984; Waychunas 1987), about the symmetry and bonding of its local environment (Bianconi 1988). The theory needed to describe XANES quantitatively is still in progress and multiple scattering calculations provided evidence to show that the number, the intensity and the shape of resonances are affected by site symmetry, bond angles and number of nearest-neighbours (Bianconi et al. 1985; Mc Keown 1989; Sainctavit et al. 1989, 1991; Cabaret et al. 1996; Wu et al. 1996). Moreover, the energies of the resonances can be related to interatomic distances (Natoli 1984). By comparison of the XANES spectra of unknown and model compounds, geometrical information about the local and intermediate-range structure of an absorbing atom can be assessed (Waychunas et al. 1983; Petiau et al. 1987; Brown et al. 1988).

In this paper, we present results of a systematic investigation of Al K-edge XANES of crystalline model compounds and phyllosilicates which complement previously published spectra of other Al-containing oxides and silicates (Brown et al. 1983; Mc Keown et al. 1985; Ildefonse et al. 1994; Li et al. 1995; Fröba et al 1995; Wu et al. 1996; Mottana et al. 1997). The objective of this work is to determine the local Al-environment in some common low-temperature minerals and to analyse the differences in Al-K XANES as a function of their chemical composition and crystallographic properties. The first part is dedicated to decriptions of the experimental setup and the materials. The second is devoted to the results: we first examine XANES spectra of crystalline model compounds, then we consider the case of 2/1 phyllosilicates and finally, we focus our attention on aluminous goethites.

Experimental and materials

Al-K XANES spectra were collected on the SA32 line at the LURE/Super-ACO facility (Orsay, France) using two α-quartz monochromator crystals (10$\bar{1}$0). The Super-ACO storage ring was operating at 800 MeV (λ_c=18.6 Å) and 100–300 mA. Great care was attributed to possible energy shift during data acquisition by recording repeatedly the same reference signal. The sample preparation consists of powder samples mounted directly on copper slides after dispersion in acetone and placement in the sample chamber under a vacuum of 10^{-5} torr. Al-K XANES spectra were collected over a photon energy range of 1550–1600 eV in 0.2 eV steps. The X-ray beam is focused on the sample using a toroidal mirror and the experimental energy resolution is of the order of 0.5 eV. These spectra include the pre-edge and near-edge features.

All Al XANES spectra were calibrated with an Al metallic foil at the inflexion point of the K-edge (1559 eV). XANES data were collected in the total electron yield mode by recording the drain current from samples onto a high purity copper substrate while the incoming flux was monitored by an ion chamber. The intensity of Al-K XANES spectra was normalized relative to the atomic absorption above the threshold and the XANES spectra were linearly background fitted so that the pre-edge regions were relatively flat. This correction facilitates direct comparison with model compounds, and from these comparisons the Al environment of unknown compounds can be "fingerprinted" in terms of differences in XANES

Table 1 Al-bearing samples examined in the present work (*LMCP* Minerals collection of the Laboratoire de Minéralogie-Cristallographie, Paris), *CN* Coordination number)

Sample	CN	Source	Composition		Reference
Berlinite	4	Synthetic	$AlPO_4$		Jumas et al. 1987
High Albite	4	location unknown	$NaAlSi_3O_8$		this study
Natrolite	4	Dakar, Senegal	$Na_2Al_2Si_3O_{10} \cdot 2\ H_2O$		this study
K-alum	6	Synthetic	$KAl(SO_4)_2 \cdot 12\ H_2O$		this study
Corundum	6	Synthetic	α-Al_2O_3		this study
Boehmite	6	Synthetic	γ-AlOOH		this study
Diaspore	6	Mougla, Turkey	α-$Al_{0.9955}Fe_{0.0045}OOH$		Hazemann et al. 1991
Kyanite	6	LMCP	Al_2SiO_5		this study
Pyrophyllite	6	Mariposa, California (Ecole des Mines, Paris)	$Al_2Si_4O_{10}(OH)_4$	Al^{IV}/Al^{tot}=0.00	this study
Gibbsite	6	Vaucluse, France	α-$Al(OH)_3$		Guendon 1981
Kaolinite	6	Decazeville, France	$Al_2Si_2O_5(OH)_4$		this study
Muscovite	4, 6	LMCP	$KAl_2(Si_3Al)O_{10}(OH)_2$	Al^{IV}/Al^{tot}=0.33	this study
Sillimanite	4, 6	LMCP	Al_2SiO_5		this study
Andalusite	5, 6	LMCP	Al_2SiO_5		this study
Smectites	4, 6	Prassa	$Na_{0.37}(Al_{1.58}Mg_{0.32}Ti_{0.01}Fe^{3+}_{0.09})\ (Si_{3.94}Al_{0.06})O_{10}(OH)_2$	Al^{IV}/Al^{tot}=0.03	D. Texier (Pers. comm.)
	4, 6	Oligocene Bassin de Paris	$Na_{0.03}K_{0.42}Ca_{0.09}(Al_{1.29}Ti_{0.04}Fe^{3+}_{0.33}Mg_{0.35})$ $(Si_{3.64}Al_{0.36})O_{10}(OH)_2$	Al^{IV}/Al^{tot}=0.22	this study
Illite/Smectite					
2M9	4, 6	Upper Silesia, Poland	88% smectite layer,	Al^{IV}/Al^{tot}=0.03	Sródon et al. 1986
2R50	4, 6	Upper Silesia, Poland	62% smectite layer,	Al^{IV}/Al^{tot}=0.08	Sródon et al. 1986
3M2	4, 6	Upper Silesia, Poland	45% smectite layer,	Al^{IV}/Al^{tot}=0.13	Sródon et al. 1986
2R63	4, 6	Upper Silesia, Poland	32% smectite layer,	Al^{IV}/Al^{tot}=0.16	Sródon et al. 1986
Illite	4, 6	Puy en Velay, France	$Na_{-0.01}K_{0.64}Ca_{0.06}(Al_{1.19}Ti_{0.04}Fe^{3+}_{0.36}Mn_{0.01}Mg_{0.43})$ $(Si_{3.53}Al_{0.47})O_{10}(OH)_2$	Al^{IV}/Al^{tot}=0.28	this study
Al-goethites	6	Synthetic series 4	$Fe_{1-x}Al_xOOH$ with x=10, 15, 20, 25, 30, 33		Goodman and Lewis 1981

(Mc Keown et al. 1985; Ildefonse et al. 1994; Wong et al. 1994; Li et al. 1995; Fröba et al. 1995). The energy position of the various edge structures has been determined using second derivative spectra. In order to estimate the relative amplitudes of edge structures, the spectra were least-squares fitted using Gaussian components, after substraction of a polynomial background due to the atomic absorption (see Ildefonse et al. 1994 for more details). This procedure was improved to assess the Al^{IV}/Al^{total} ratio in amorphous alumino-silicates, in comparison with ^{27}Al MAS NMR.

Four-fold aluminium crystalline model compounds are albite, natrolite and berlinite. In albite, aluminium atoms are in four different tetrahedral sites with point symmetry 1. In berlinite and natrolite, there is one aluminium site, respectively with point symmetry 2 and 1. Six-fold aluminium model compounds are K-alum, corundum, boehmite, diaspore, pyrophyllite, kyanite, gibbsite, kaolinite. The first five materials are characterized by one octahedral site with various point symmetry (from *m*3*m* in K-alum to 1 pyrophyllite). In kyanite, aluminium atoms are in four octahedral sites (point symmetry 1) and in gibbsite and kaolinite, they are in two octahedral sites (point symmetry 1). Muscovite and sillimanite are model compounds for minerals containing both six-fold and four-fold Al, and andalusite is a model compound with both five- and six-fold aluminium.

Low temperature clay minerals investigated in this study include 2/1 phyllosilicates (illite, smectites), mixed layers minerals belonging to illite/smectite group, and synthetic aluminous goethites (series 4 prepared from Fe(II) path at T=25°C, Goodman and Lewis 1981), for which Al-contents vary between 10 and 33 mol% AlOOH.

All samples have been studied by XRD to assure their purity. Table 1 presents their origin and composition.

Results and spectral interpretation

Crystalline model compounds

Four-fold coordinated Al

Figure 1 displays Al K-XANES spectra of albite, natrolite and berlinite, and Table 2 summarizes the energy positions of the resonances as well as the mean Al^{IV}-O distances. The experimental spectrum of albite consists of a strong single-edge maximum (A) at 1565.4 eV (1.5 eV wide) and four ill-defined features at 1569.5 (B), 1573.5 (C), 1579 (D), and 1583.0 eV (E). The strong edge feature A is related to a 1*s* to 3*p* transition in the μ_o (absorption cross-section) for Al (Mc Keown 1989; Cabaret et al. 1996). The spectrum of berlinite, $AlPO_4$, shows a strong edge maximum at 1566.8 eV (1.5 eV wide) and four ill-defined structures at 1570.5, 1574.6, 1577.0 and 1584.0 eV. The Al-K XANES spectrum of natrolite yields a strong edge maximum at 1566.4 eV (1.5 eV wide) and three poorly resolved features at 1572.0, 1575.0 and 1583.0 eV. Few differences are then observed between the XANES spectra of these three reference compounds for Al^{IV} in a low site symmetry (2) and (1). The main characteristic of XANES for tetrahedral Al is the presence of an intense white line (2 eV wide) located between 1565.4 and 1566.8 eV, which represents about 100% of the atomic absorption. The highest energy value (1566.8 eV) is from berlinite, where Al has P as a second neighbour, and this has a higher electronegativity than Si (in albite and natrolite). That induces a decrease of the electronic density around oxygen and is responsible for the shift of the main absorption feature towards the highest energies. Differences between spectra concern mainly the structures observed above the main absorption edge feature. These resonances, labelled B, C and D, have low amplitudes and are related to medium range order due to multiple scattering from several atomic shells, as has been demonstrated for berlinite and natrolite (Cabaret et al. 1996). By contrast, A and E resonances have been partly related to the first coordination sphere (5 atom cluster calculation by Cabaret et al. 1996).

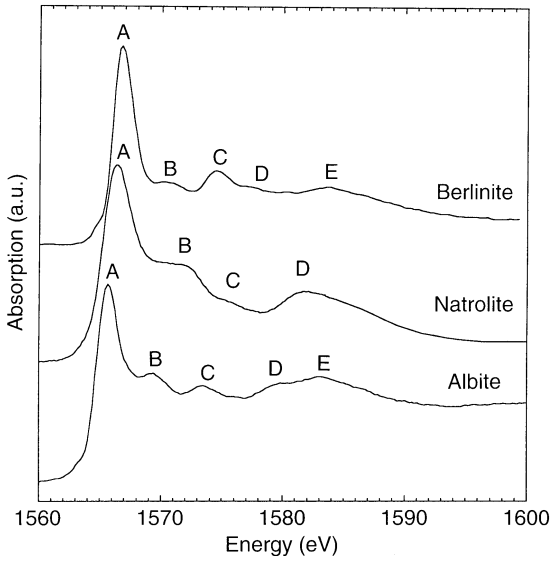

Fig. 1 K-Al XANES of crystalline model compounds for four-fold aluminium

Six-fold coordinated Al

Experimental Al K-XANES spectra of six-fold coordinated aluminium compounds are plotted on Fig. 2. The energy positions of the resonances as well as the mean Al^{VI}-O distances are listed in Table 3. The XANES spectrum of α-Al_2O_3 (corundum) contains five features in the first 15 eV. The first one, located on the low energy side of the absorption edge (A' component at 1565.4 eV) has a weak intensity. The second feature (A), at 1567.4 eV (1.5 eV wide) and highest in intensity, represents about 250% of the atomic absorption. A and B resonances are separated by a small plateau. The three others features, B, C and D, at higher energies (1571.6, 1573.1 and 1576 eV) have been related on one hand to shape resonances due to full scattering effects (single and multiple scattering) from several shells beyond the octahedral "core" (Mc Keown 1989), and on another hand to the electronic structure of corundum (Cabaret et al. 1996). In corundum, octahedral Al is surrounded by six nearest oxygen neighbours at 1.849 and 1.980 Å, and four near nearest Al neighbours at 2.65 and 2.79 Å (Newnham and de Haan 1962). In contrast to the spectra of four-fold

Table 2 Positions in energy of main Al-K edge structures in XANES spectra and mean Al^{IV}-O distances for four-fold Al in crystalline model compounds

Sample	A	B	C	D	E	Al^{IV}-O
Albite	1565.4	1569.5	1573.5	1579	1583	1.742 (Kroll and Ribbe 1983)
Natrolite	1566.4	1572.5	1575		1583	1.709 (Alberti et al. 1995)
Berlinite	1566.8	1570.5	1574.6	1577	1584	1.738 (Schwarzenbach 1966)

Table 3 Positions in energy of main Al-K edge features in XANES spectra and mean Al^{VI}-O distances for six-fold Al in crystalline model compounds

Sample	A	B	Al^{VI}-O
K-Alum	1567.8	1572.2	1.908 (Larson and Cromer 1967)
Corundum	1567.4	1571.6	1.914 (Newnham and de Haan 1962)
Boehmite	1567.6	1571.6	1.907 (Corbato et al. 1985)
Diaspore	1567.4	1571.6	1.915 (Busing and Levy 1958)
Kyanite	1567.4	1571.4	1.907 (Winter and Ghose 1979)
Gibbsite	1567.6	1571.4	1.902 (Saalfeld and Wedde 1974)
Kaolinite	1568.2	1570.8	1.914 (Bish and van Dreele 1989)
Pyrophyllite	1567.8	1571.2	1.912 (Lee and Guggenheim 1981)

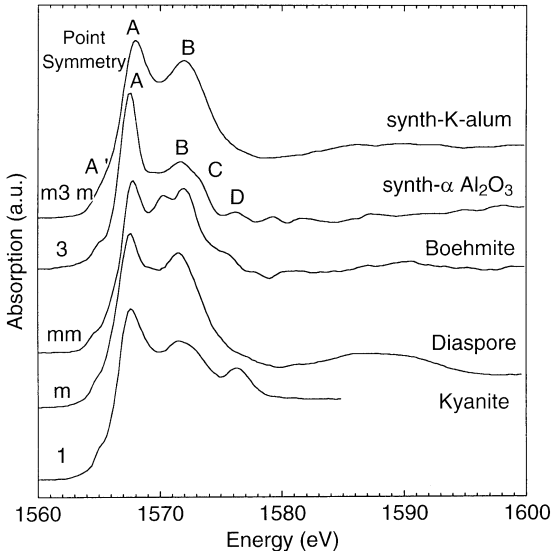

Fig. 2 K-Al XANES of crystalline model compounds for six-fold aluminium. Spectra are presented with respect to the point symmetry of the octahedron containing Al

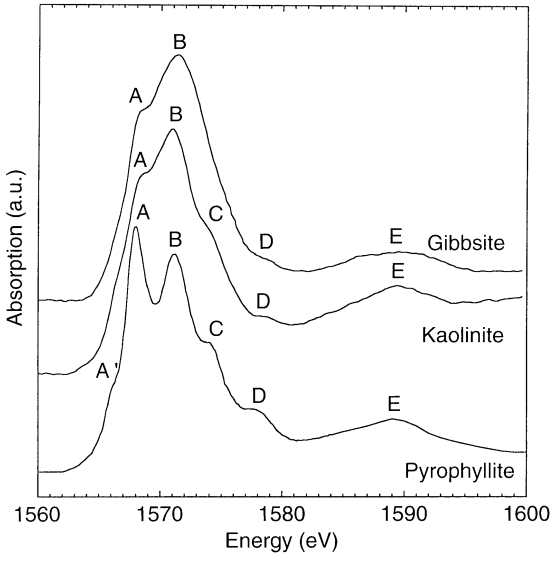

Fig. 3 K-Al XANES of crystalline model compounds for six-fold aluminium in a dioctahedral layer

coordinated Al, XANES spectra of six-fold coordinated Al show much more complex features and shifts in amplitude from material to material (Figs. 2, 3).

The XANES spectrum of K-alum, $KAl(SO_4)_2.12H_20$, contains two main edge maxima at 1567.8 (A) and 1572.2 eV (B), this second resonance being symmetric in contrast to the spectrum of corundum where two components are clearly resolved (B and C resonances in Fig. 2). K-alum has one octahedral site in a cubic symmetry with six nearest H_2O neighbours at 1.908 Å and six next nearest H_2O neighbours at 2.690 Å (Larson and Cromer 1967). The XANES of K-alum may be considered as a reference model for an Al surrounded by 6 H_2O molecules in a symmetric octahedron. The simulation performed by Cabaret et al. (1996) for a 7 atom cluster (Al absorber and 6 nearest oxygen neighbours in O_h symmetry) yields only one spectral feature corresponding to peak A. The occurrence of the second resonance B in K-alum has to be related to multiple scattering processes from several atomic shells around the absorber.

The XANES spectrum of boehmite, γ-AlOOH, yields three edge maxima and a shoulder at higher energy. The feature with the highest amplitude is located at 1567.6 eV and is followed by two resonances with a lower amplitude at 1570.2 and 1571.6 eV. A shoulder is also resolved at 1575 eV. Boehmite contains one Al in a distorted octahedron with point symmetry *mm* and three groups of Al-O distances at 1.949, 1.895 and 1.877 Å (Corbato et al. 1985).

The XANES spectrum of diaspore, α-AlOOH, is similar to that of corundum, presenting two main absorption features at 1567.4 and 1571.2 eV separated by a small plateau. The second feature is nearly symmetric although the Al containing octahedra are significantly distorted. In diaspore, Al is located in one octahedral site with point symmetry *m* and there are two groups of Al-O average

distances at about 1.977 and 1.855 Å (Busing and Levy 1958). As for corundum, simulation of the XANES spectrum of diaspore has to take into account large clusters (15 Å in diameter) which means that medium range order is reflected by the Al-K XANES spectra. As an example, the A' feature observed at low energy in all spectra of Fig. 2, is only present in simulations when clusters larger than 12 Å are considered (Cabaret et al. 1996).

The XANES spectrum of kyanite, Al_2SiO_5, yields three maxima. The highest in amplitude is located at 1567.4 eV and is followed by an asymmetric resonance at 1571.4 eV (with a shoulder at 1572.4 eV) and by a resonance at 1576.1 eV, the lowest in intensity. Kyanite is characterized by four very distorted octahedral sites with a range of Al-O distances spread over 1.816 to 1.998 Å (Winter and Ghose 1979).

Figure 3 presents the XANES spectra of reference model compounds having a low site symmetry (1) and with octahedra linked by the edge to form a layer where only 2/3 of octahedral sites are occupied by Al.

The XANES spectrum of gibbsite consists of a broad peak (8 eV wide) where two main absorption features can be distinguished, the first one (A) located at 1567.6 eV and the second one (B), very broad and more intense, at 1571.4 eV. Gibbsite consists of octahedral layers with two Al sites located in very distorted octahedra: Al-O distances spread over 1.832 to 1.947 Å (Saalfeld and Wedde 1974).

The XANES spectrum of a well ordered kaolinite, $Al_2Si_2O_5(OH)_4$, is close to that of gibbsite, the main feature being narrower (6 eV wide), and presents six distinguishable features. At 1566 eV, a shoulder A' may be related to a pre-edge feature as that observed in corundum, but having a higher amplitude in kaolinite. The second feature (A) is located at about 1568.2 eV and is less intense than the feature B at 1570.8 eV. The fourth feature (C) consists of a shoulder at higher energy around 1573 eV. At higher energies, D and E resonances occur at 1578 and 1589 eV respectively. Kaolinite like gibbsite has two Al sites in very distorted octahedra where Al-O distances are between 1.880 and 1.969 Å without resolved mode (Bish and von Dreele 1989). In kaolinite, the gibbsite-like layer is associated to a tetrahedral layer containing Si, which constitutes the third shell beyond a central Al (two Si at 3.143 and 3.256 Å).

The XANES spectrum of pyrophyllite, $Al_2(Si_4O_{10})(OH)_2$, consists also of six features. At 1566 eV, a weak pre-edge feature (A') is present. The second feature (A), at 1567.8 eV (2 eV wide), has the highest amplitude and is clearly separated from the third B feature, still quite narrow, at 1571.2 eV. The fourth feature (C) consists of a weak amplitude peak at 1574.0 eV. D and E resonances

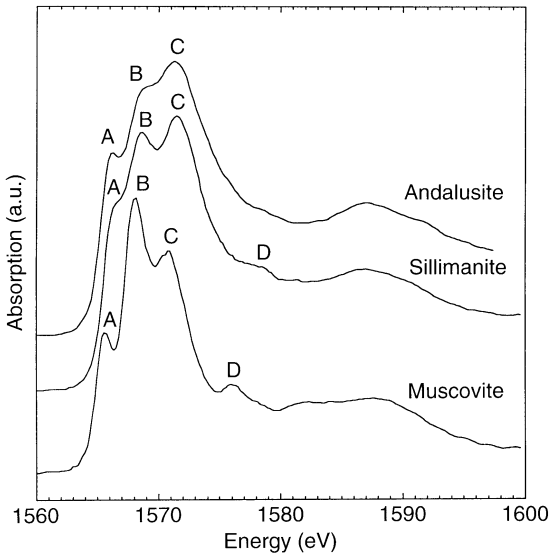

Fig. 4 K-Al XANES of crystalline model compounds with mixed CN for Al. (Four- and six-fold Al: muscovite and sillimanite. Five- and six-fold Al: andalusite)

are at the same energies as in kaolinite, but the amplitude of the D resonance is higher than that in kaolinite and gibbsite. In contrast to gibbsite and kaolinite, pyrophyllite has only one distorted octahedral site and Al-O distances may be grouped in two sets at about 1.92 and 1.88 Å (Lee and Guggenheim 1981). In pyrophyllite, the gibbsite-like layer is sandwiched between two tetrahedral layers containing silicon, and four Si constitute a third shell beyond the central Al.

All XANES spectra of the reference model compounds for six-fold Al yield a feature A which is quite constant in energy, between 1567.4 eV in diaspore and 1568.2 eV in kaolinite. The most significant changes among these spectra occur at higher energies and affect shape, number and shift in energy of XANES features. We have established that when considering poorly symmetric structures (point symmetry 1), significant changes in XANES are observed; for example between gibbsite and kaolinite on the one hand, and pyrophyllite on the other hand.

Mixed coordination number in reference compounds

The XANES spectra of muscovite, sillimanite and andalusite, which serve as crystalline model compounds for mixed CN in minerals, contain three main features (Fig. 4, Table 4).

In the muscovite spectrum, the first resonance (A) is narrow (2 eV) and located at 1565.4 eV, the second (B)

Table 4 Positions in energy of main Al-K edge structures in XANES spectra and mean Al^{VI}-O distances for four-, five- and six-fold Al in crystalline model compounds

Sample	A	B	C	Al^{VI}-O
Muscovite	1565.4	1567.8	1571.0	1.930 (Rothbauer 1971)
Sillimanite	1565.0	1566.8	1570.4	1.912 (Winter and Ghose 1979)
Andalusite	1565.0	1567.6	1570.4	1.935 (Winter and Ghose 1979)

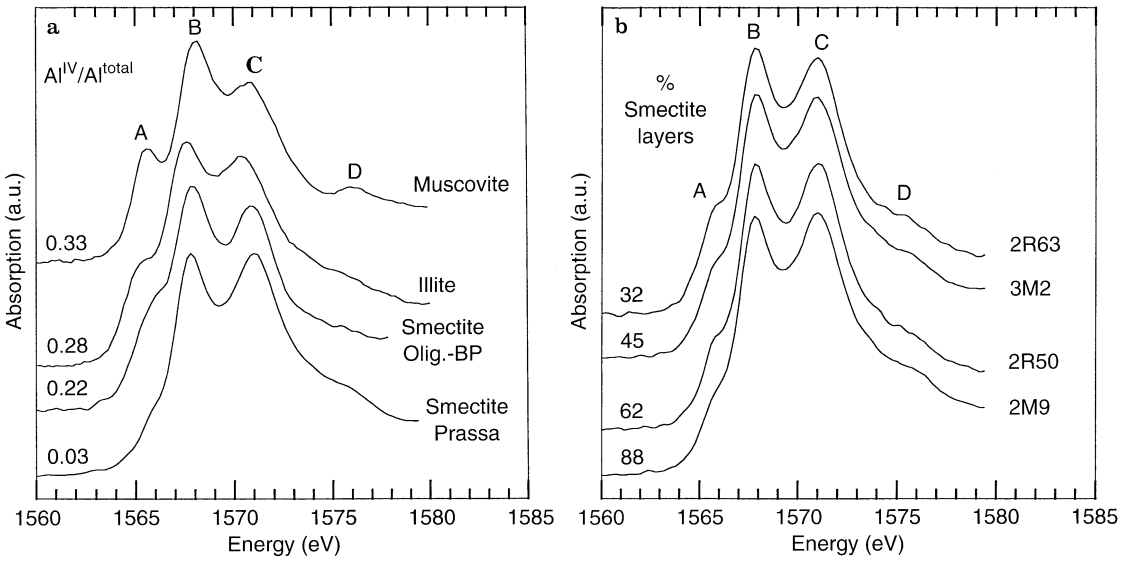

Fig. 5a, b **a** K-Al XANES of dioctahedral 2/1 phyllosilicates (micas and smectites). Spectra are sorted as a function of the Al^{IV}/Al^{total} ratio. **b** K-Al XANES of dioctahedral illite/smectite mixed layers minerals. Spectra are sorted as a function of the % of smectite layers

is also narrow (2 eV) and more intense at 1567.8 eV and the third (C), which is asymmetric and has an intermediate amplitude, is located at 1570.8 eV. In sillimanite, XANES yields quite similar features but feature C at 1571.4 eV has the highest amplitude while the structure A at 1566 eV is weakly separated from the second broad B resonance at 1568.4 eV.

The XANES of andalusite presents also three narrow and resolved resonances at 1565.8, 1568.3 and 1571.7 eV.

By analogy with the XANES of reference compounds for four- and six-fold Al, and since the spectra of muscovite, sillimanite and andalusite yield sufficiently narrow resolved resonances, we develop the following fingerprint approach. Since the six-fold coordinated Al gives origin to the feature located around 1570 eV, one can say, with reasonable confidence, that the first feature (A) at lower energy may be related to four-fold Al in muscovite and sillimanite, and to five-fold Al in andalusite. The origin of the B resonance is still a puzzle that can only be solved by careful calculation. The resonance C, at higher energy may be mainly related to six-fold Al. These interpretations of the spectra differs from that of Li et al. (1995). These authors related the B feature to five-fold Al in andalusite, although this feature is at the same energy as that for sillimanite. They did not consider the low energy shoulder in their spectrum which occurs as in our spectrum at the energy of the A resonance in sillimanite and in muscovite. One important point for us is that some of their spectra are much different from ours without any sensible explanation.

The 2 eV shift between the first and the second resonance, related to four- and/or five- and to six-fold aluminium respectively, makes Al-K XANES a fingerprinting method for the determination of Al-CN, as previously stated by Brown et al. (1983), Mc Keown et al. (1985), Mc Keown (1989), Ildefonse et al. (1994), Wong et al. (1994), Li et al. (1995), Fröba et al. (1995), Mottana et al. (1997). However four- and five-fold Al cannot be distinguished in the reference compounds studied.

2/1 phyllosilicates: estimation of Al^{IV}/Al^{total}

The Al-K XANES spectra of a suite of dioctahedral 2/1 phyllosilicates have been recorded: pyrophyllite (Fig. 3), two smectites and two micas (illite and muscovite) (Fig. 5a). All samples present the same low point symmetry (1) and only one octahedral site. Pyrophyllite and muscovite represent two end members with no structural charge (Al^{IV}/Al^{total}=0) and one charge (Al^{IV}/Al^{total}=0.33) respectively. In Fig. 5a, XANES spectra are presented according to the amount of four-fold Al estimated by calculation from chemical analysis. All the XANES spectra yield two main absorption features, B and C. At lower energy, the first feature (A) (1565.6–1566.0 eV) sees its amplitude increased as Al^{IV}/Al^{total} ratio increases in the samples studied. The second feature (B), the most intense, varies in energy position between 1567.6 and 1568.0 eV. The third feature (C), at higher energy (1570.6–1571.0 eV), is quite broad.

A second set of dioctahedral phyllosilicates has been studied. It consists of four illite/smectite mixed layers, presenting a range of 32 to 88% smectite layers as determined by XRD (Srodòn et al. 1986). XANES spectra of these four samples are presented on Fig. 5b. They are very similar in shape to other dioctahedral phyllosilicates studied above, and two main features are always distinguishable with constant position in energy at 1567.8 eV for B and 1571.0 eV for C. These two main structures, B and C, indicate that aluminium in these mixed-layer minerals is mainly in octahedral coordination, and the low energy shoulder (A component at 1566 eV) increases in amplitude as the illite content increases in the studied samples. This change is in agreement with the montmorillonitic character of the smectitic layers in mixed layers illite/

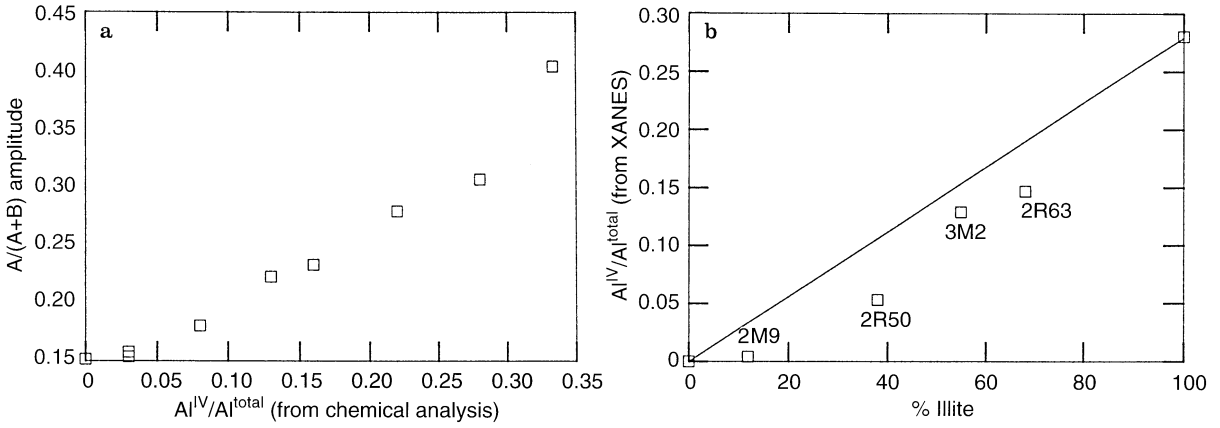

Fig. 6a, b **a** Relation between the calculated Al^{IV}/Al^{total} ratio from the chemical analysis and the A/(A+B) amplitude ratio from XANES of 2/1 dioctahedral clay minerals studied. **b** Relation between the Al^{IV}/Al^{total} ratio estimated from the XANES data and the % of illite layers calculated from XRD

smectite and with the increasing illitic layers, which contain four-fold Al (Srodòn et al. 1986).

Since A, B and C resonances occur at energy values which are very close from one sample to another, and since the amplitude of the first resonance (A) increases as Al^{IV}/Al^{total} ratio increases, XANES could be used for the assessment of Al^{IV}/Al^{total} ratios in these phyllosilicates. Decomposition of the spectra in gaussian components has been carried out for a better estimation of the A/A+B amplitude ratios (Ildefonse et al. 1994). There is a good quantitative correlation between the intensity of the XANES feature for four-fold Al (estimated as presented above) and Al^{IV}/Al^{total} determined from chemical analysis for these two sets of phyllosilicate samples (Fig. 6a). At high Al^{IV}/Al^{total} ratios (muscovite), the relationship is not linear. Since the spectrum of pyrophyllite also yields a feature at the same energy as that of four-fold Al, and in order to obtain the signal for Al^{IV}, we corrected the A/A+B amplitude ratios of illite/smectite mixed layers by the same value measured in pyrophyllite, which contains only six-fold Al. If we consider illite and pyrophyllite as end members for Al^{IV}/Al^{total}=0.28 and 0 respectively, the amplitude of the A feature (at 1566 eV) may be used to calculate the Al^{IV}/Al^{total} of illite/smectite mixed layers. We compare the derived Al^{IV}/Al^{total} values to the %illite layers calculated by XRD (Fig. 6b). The straight line is the ideal correlation based on the Al^{IV}/Al^{total} in pyrophyllite and illite. All points depart from the straight line. This discrepancy could be related to the overestimation of illite layers measured by XRD. This trend is in agreement with TEM data obtained on illite/smectite minerals, which indicate that the XRD determination of smectite layers has to be increased when considering that the edges of particles are made of smectitic interlayers (Srodòn et al. 1990).

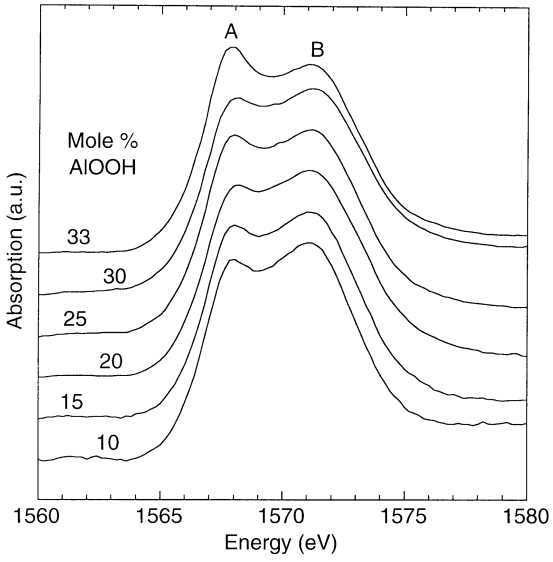

Fig. 7 K-Al XANES of synthetic Al-goethites. Spectra are sorted as a function of their mol% of AlOOH

Local Al environment in $Fe_{1-x}Al_xOH$

Goethite and diaspore have the same structure (space group *Pnma*) and a partial solid-solution is known to exist between these two minerals. Al-goethites are widespread weathering minerals in lateritic soils. Up to 33 mol% of AlOOH can substitute for Fe (Fitzpatrick and Schwertmann 1982). In diaspore, only 15 mol% of FeOOH is known (Hazemann et al. 1991). XANES spectra of synthetic Al-goethites (10 to 33 mol% of AlOOH) are presented on Fig. 7.

Significant differences are observed between spectra, which may be distinguished according to the energy position and the respective amplitude of the two main resonances, A and B. On the spectrum corresponding to 10 mol% of AlOOH, A and B features are located at 1567.9 and 1571.1 eV respectively. As the AlOOH mole ratio increases to 33%, peak A is shifted to lower energy while peak B is shifted to higher energy. Thus the separation between the two features increases, and becomes in agreement with that observed in the diaspore case (see Table 3).

At low Al concentrations, the low energy feature is less intense than that at higher energy. When the Al increases in goethite, the respective amplitude of the low energy feature increases and for the 33 mol% sample the low energy feature has the highest amplitude (Fig. 7).

We have performed full multiple scattering calculations for diaspore with the goethite crystallographic parameters. We found that this model is unable to reproduce the spectral modifications with concentration. Then the reduction of peak A and the decrease of energy separation between A and B come from the electronic modifications due to the Al substitution for Fe. In diaspore, as well as in goethite, cations (Al and/or Fe) are in a single octahedral site. Each octahedron shares an edge with four neighbouring octahedra and a double corner with four neighbouring octahedra. For low Al-concentrations, Al-K XANES spectra of Al-goethites are more similar to that of gibbsite (Fig. 3) than that for diaspore (Fig. 2). At low Al-concentration, substituted Al may be mainly located in octahedra which share only edges with their near neighbours as in gibbsite. At higher concentrations, Al could be distributed in edge-sharing and corner-sharing octahedra as in diaspore. This assumption has to be verified by full multiple scattering calculations which are in progress and beyond the scope of this paper.

Conclusions

Determination of the CN of aluminium

XANES is a fingerprinting method for the determination of the coordination number of aluminium in minerals. A 2 eV shift distinguishes the four-fold and the six-fold Al, but all minerals with only six-fold aluminium yield a low amplitude feature located at the same energy as that of the main absorption feature for four-fold Al. Nevertheless, quantitative determination of Al^{IV}/Al^{total} ratios in unknown samples can be performed provided that a close reference compound containing only six-fold Al is available. In allophanes, such a procedure was done by using imogolite (Ildefonse et al. 1994), and in the present paper pyrophyllite was used as a reference compound for 2/1 phyllosilicates. Four-fold Al can be detected in clay minerals provided that a good background subtraction is done. As little as 3% four-fold Al can be observed. There is also a monotonic relationship between the intensity of the feature due to four-fold Al and the Al^{IV}/Al^{total} ratios determined by chemical analysis.

Sensitivity to octahedral point symmetry

XANES spectra of six-fold Al differ with different Al-site symmetry. Following Mc Keown et al. (1985), one can notice that for the selected compounds of Fig. 2, XANES features which increase in number and decrease in amplitude as site symmetry decreases from K-alum to kyanite. Although compounds with similar environment with high symmetry are expected to be almost identical, one observes in Fig. 3 that low symmetry Al can obviously yield very different spectral features.

Sensitivity to number of Al sites and to second neighbours

The differences in K-Al XANES of minerals having Al point symmetry 1 may be related to the number of aluminium sites and to the influence of the second neighbours. For minerals having only one Al site (pyrophyllite, dioctahedral micas, smectites and illite/smectite), the two edge maxima are clearly separated and the edge maximum is located at low energy near 1568 eV. For minerals having two Al sites (kaolinite-group minerals and gibbsite), there is a large XANES feature with a maximum at higher energy near 1570 eV. These differences may be rationalized using the results of Garcia et al. (1986) for octahedral aqueous complexes of transition metal cations, and those of Cabaret et al. (1996) for Al oxides and silicates. These authors have shown using multiple scattering calculations that the B structure is determined by a full multiple scattering resonance where all multiple scattering contributions to the total cross section are in phase. When two Al^{VI}-sites are present, such as in gibbsite and kaolinite, the probability of constructive multiple scattering contributions decreases because of the distribution of site symmetry and interatomic distances. As a consequence, the amplitude of the B resonance decreases.

A gibbsitic octahedral layer can be considered as a prototype octahedral sheet for clay minerals, but the Al-K XANES spectra of gibbsite and dioctahedral phyllosilicates (2/1 and 1/1) are significantly different. These spectra are very sensitive to the second neighbouring atoms of aluminium: in gibbsite, edge sharing octahedra constitutes a dioctahedral layer (only two out of three octahedral sites are occupied), in 1:1 phyllosilicates (kaolinite-group minerals) a gibbsitic sheet is linked to a tetrahedral layer, and in 2:1 phyllosilicates (pyrophyllite, micas, smectites) a gibbsitic sheet is sandwiched between two tetrahedral layers. Moreover, for these last minerals, the number of Al sites may be more important as discussed above. Thus, contributions of atomic shells beyond the octahedral oxygens must be taken into account for a better understanding of the XANES features.

Multiple scattering effects

Careful interpretation of XANES spectra requires theoretical calculations. Several attempts have been made to simulate and interpret Al-K XANES spectra. The pioneering work was performed by Mc Keown (1989) who made calculations on small clusters (16 atoms at maximum). Although the agreement between experimental and calculted spectra were still poor, he demonstrated that multiple scattering processes have to be taken into account for explaining the high energy features. More recently, Li et al. (1995) interpreted the Al-K XANES spectra of reference

compounds by using results obtained on Si-compounds where resonances features were related to electronic transitions according to molecular orbital theory. The transposition of Si data to Al data is not strictly valid since the electronic configuration of Al is different from that of Si. Besides, for six-fold Al compounds, XANES features were assigned to electronic transitions assuming an O_h symmetry for the octahedron whereas all studied compounds have distorted octahedral sites and then symmetry lower than O_h. Finally, recent calculations of Al-K XANES spectra have been performed by using the full multiple scattering method (Natoli et al. 1980) on large clusters (40–100 atoms). They have shown that for both four-fold and six-fold Al in reference compounds (berlinite, natrolite, corundum, diaspore, garnets), resonances above the white line were characterized by multiple scattering effects and medium range order (Cabaret et al. 1996; Wu et al. 1996). Calculations proved that, for the Al K-edge, the mean free path of the photoelectron is larger than 30 Å.

Since EXAFS at Al-K edge is difficult in silicates due to the limited energy range probed, XANES is a powerful method for understanding structural changes in amorphous compounds and in poorly ordered minerals present in low temperature environments at Earth's surface provided that simulations of spectra could be extended to disordered systems.

Acknowledgements We are indebted to Dr Srodòn for supplying the four illite/smectite samples, to Dr Tessier for providing Prassa smectite samples, to Dr Prost for providing illite sample, and to Professor U. Schwertmann for providing the synthetic Al-goethites. The staff of LURE is acknowledged for valuable assistance. This paper was improved thanks to the suggestions of two anonymous referees. This study has been supported by CNRS INSU (Contribution DBT# 93–000; Ph. I.) and IPGP (contribution 283).

References

Alberti A, Cruciani G, Dauru I (1995) Order-disorder in natrolite group minerals. Eur J Mineral 7:501–508

Bianconi A (1988) XANES spectroscopy. In: Koningsberger DC, Prins R, X-ray absorption: principles, applications, techniques of EXAFS, SEXAFS and XANES. Wiley, New York, pp 573–662

Bianconi A, Fritsch E, Calas G, Petiau J (1985) X-ray absorption near-edge structure of 3d transition elements in tetraedral coordination. The effect of bond-length variation. Phys Rev B 32:4292–4295

Bish DL, Von Dreele RB (1989) Rietveld refinement of non-hydrogen atomic positions in kaolinite. Clays Clay Minerals 37:289–296

Brown GE Jr, Parks G (1989) Synchrotron-based X ray absorption studies of cation environments in Earth materials. Reviews in Geophysics 27:519–533

Brown GE Jr, Dikmen FD, Waychunas GA (1983) Total electron yield K-XANES and EXAFS investigation of aluminum in amorphous aluminosilicates. Report 83/01, Stanford Synchrotron Radiat. Lab., Stanford California, pp 146–147

Brown GE Jr, Calas G, Waychunas GA, Petiau J (1988) X-ray absorption spectroscopy: applications in mineralogy and geochemistry. In: Hawthorne FC Spectroscopic methods in mineralogy and geology (Reviews in Mineralogy vol. 18). Mineralogical Society of America, Washington DC, pp 431–512

Busing WR, Levy HA (1958) A single crystal neutron diffraction study of diaspore, AlO(OH). Acta Crystallogr 11:798–803

Cabaret D, Sainctavit Ph, Ildefonse Ph, Flank A-M (1996) Full multiple scattering calculations on silicates and oxides at Al-K edge. J Phys: Condens. Matter 8:3691–3704

Calas G, Petiau J (1983) Coordination of iron in oxide glasses through high resolution K-edge spectra: information from the pre-edge. Solid State Commun 48:625–629

Corbato CE, Tettenhorst RT, Christoph GG (1985) Structure refinement of deuterated boehmite. Clays Clay Minerals 33:71–75

Fitzpatrick RW, Schwertmann U (1982) Al-substituted goethite – an indicator of pedogenic and other weathering environments in South Africa. Geoderma 27:335–347

Fröba M, Wong J, Rowen M, Brown Jr GE, Tanaka T, Rek Z (1995) Al and Si K absorption edges of Al_2SiO_5 polymorphs using the new YB_{66} soft X-ray monochromator. Physica B 208&209:555–556

Galoisy L, Calas G, Brown GE Jr (1995) Intracrystalline distribution of Ni in San Carlos olivine: an EXAFS study. Am Mineral 80: 1089–1092

Garcia J, Bianconi A, Benfatto M, Natoli CR (1986) Coordination geometry of transition metal ions in dilute solutions by XANES. J Phys (Paris) Colloq C8 47:49–54

Goodman BA, Lewis DG (1981) Mössbauer spectra of aluminous goethites (αFeOOH). J Soil Sci 32:351–363

Guendon JL (1981) Le paleokarst du Coulon (Vaucluse, France). Sédimentation et altération d'une série détritique sur substratum carbonaté: karstification sous couverture, accumulation de gibbsite, paléosols. PhD dissertation, Marseille

Hazemann JL, Manceau A, Sainctavit Ph, Malgrange C (1991) Structure of the αFeOOH solid solution. I. Evidence by polarized EXAFS for an epitaxial growth of hematite-like-clusters in diaspore. Phys Chem Minerals 19:25–38

Ildefonse Ph, Kirkpatrick RJ, Montez B, Calas G, Flank A-M, Lagarde P (1994) Al MAS NMR and aluminium X-ray absorption near edge structure study of imogolite and allophanes. Clays Clay Minerals 42:276–287

Jumas JC, Goiffon A, Capelle B, Zarka A, Doukhan JC, Schwartzel J, Détaint J, Philippot E (1987) Crystal growth of berlinite, AlPO4: physical characterization and comparison with quartz. J Cryst Growth 80:133–148

Kirkpatrick RJ (1988) MAS NMR spectroscopy of minerals and glasses. In: Hawthorne FC Spectroscopic methods in mineralogy and geology (Reviews in Mineralogy vol. 18). Mineralogical Society of America, Washington DC, pp 341–403

Kroll H, Ribbe PH (1983) Lattice parameters, composition and Al,Si order in alkali feldspars. In: Ribbe H (ed) Feldspar mineralogy (Reviews in Mineralogy vol. 2). Mineralogical Society of America, Washington DC, pp 57–99

Larson AC, Cromer DT (1967) Refinement of the alum structures. III. X-ray study of the αalums, K, Rb and $NH_4Al(SO_4)_2.12H_2O$. Acta Cryst 22:793–800

Lee JH, Guggenheim S (1981) Single crystal X-ray refinement of pyrophyllite-1*Tc*. Am Mineral 66:350–357

Li D, Bancroft M, Fleet ME, Feng XH, Pan Y (1995) Al-K edge XANES spectra of aluminosilicate minerals. Am Mineral 80:432–440

Mc Keown DA (1989) Aluminum X-ray absorption near edge spectra of some oxide minerals: calculation versus experimental data. Phys Chem Minerals 16:678–683

Mc Keown DA, Waychunas GA, Brown GE (1985) EXAFS study of the coordination environment of aluminum in a series of silica-rich glasses and selected minerals within the Na_2O-Al_2O_3-SiO_2 system. J. Non-Cryst Solids 74:349–371

Mottana A, Robert JL, Marcelli A, Giuli G, Della Ventura G, Paris E, Wu Z (1997) Octahedral vs. tetrahedral Al coordination in synthetic micas by XANES spectroscopy. Am Mineral 82:497–502

Natoli CR (1984) Distance dependence of continuum and bound state of excitonic resonances in x-ray absorption near edge structures (XANES). In: Hodgson KO, Hedman B, PennerHahn JE

EXAFS and near edge structure III. (Springer Proc. Physics 2). Springer Berlin, pp 38–42
Natoli CR, Misemer DK, Doniach S, Kutzler FW (1980) First-principles calculations of X-ray absorption edge structure in molecular clusters. Phys Rev A 22:1104–1108
Newnham RE, de Haan YM (1962) Refinement of α-Al_2O_3, Ti_2O_3, V_2O_3 and Cr_2O_3 structures. Z Kristallogr 117:235–237
Petiau J, Calas G, Sainctavit Ph (1987) Recent developments in the experimental studies of XANES. J Phys C9 48:1085–1096
Rothbauer VR (1971) Untersuchung eines $2M_1$-Muskovits mit Neutronenstrahlen. N Jahrb Mineral Mh 143–154
Saalfeld H, Wedde M (1974) Refinement of the crystal structure of gibbsite, $Al(OH)_3$. Z Kristallogr 139:129–135
Sainctavit Ph, Petiau J, Benfatto M, Natoli CR (1989) Comparison between XAFS experiments and multiple-scattering calculations in silicon and zincblende. Physica B158:347–355
Sainctavit Ph, Petiau J, Laffon C, Flank A-M, Lagarde P (1991) Structural properties extracted from multiple-scattering calculations in silicon carbide nanocrystallites. In: Hasnain SS X-ray absorption fine structure. Ellis Horwood, Chichester pp 38–40
Schwarzenbach von D (1966) Verfeinerung der Struktur der Tiefquarz-Modifikation von $AlPO_4$. Z Kristallogr 123:161–185
Srodòn J, Morgan DJ, Eslinger EV, Eberl D, Karlinger MR (1986) Chemistry of illite/smectite and end-member illite. Clays Clay Minerals 34:368–378
Srodòn J, Andreoli C, Elsass F, Robert M (1990) Direct high-resolution transmission electron microscopic measurement of expandability of mixed-layer illite/smectite in bentonite rock. Clays Clay Minerals 38:373–379
Waychunas GA (1987) Synchrotron radiation XANES spectroscopy of Ti in minerals: effects of Ti bonding distances, Ti valence and site geometry on absorption edge structure. Am Mineral 72:89–101
Waychunas GA, Apted MJ, Brown GE Jr (1983) X-ray absorption spectra of Fe minerals and model compounds: near edge structure. Phys Chem Minerals 10:1–9
Winter JK, Ghose S (1979) Thermal expansion and high-temperature crystal chemistry of the Al_2SiO_5 polymorphs. Am Mineral 64:573–586
Wong J, Lytle FW, Messner RP, Maylotte DH (1984) K-edge absorption spectra of selected vanadium compounds. Phys Rev B 30:5596–6510
Wong J, George GN, Pickering IJ, Rek ZU, Rowen M, Tanaka T, Via GH, De Vries B, Vaughan DEW, Brown Jr GE (1994) New opportunities in XAFS investigation in the 1–2 keV region. Solid State Commun 92:559–562
Wu Z, Marcelli A, Mottana A, Giuli G, Paris E, Seifert F (1996) Effects of higher-coordination shells in garnets detected by x-ray-absorption spectroscopy at the Al K-edge. Phys Rev B 54:2976–2979